CHANNELS
2016, VOL. 10, NO. 5, 379–394
http://dx.doi.org/10.1080/19336950.2016.1180489

Taylor & Francis
Taylor & Francis Group

RESEARCH PAPER

OPEN ACCESS

Similar molecular determinants on Rem mediate two distinct modes of inhibition of $Ca_V1.2$ channels

Akil A. Puckerin[a], Donald D. Chang[b], Prakash Subramanyam[b], and Henry M. Colecraft[a,b]

[a]Department of Pharmacology & Molecular Signaling, Columbia University, New York, NY, USA; [b]Department of Physiology & Cellular Biophysics, Columbia University, New York, NY, USA

ABSTRACT

Rad/Rem/Rem2/Gem (RGK) proteins are Ras-like GTPases that potently inhibit all high-voltage-gated calcium (Ca_V1/Ca_V2) channels and are, thus, well-positioned to tune diverse physiological processes. Understanding how RGK proteins inhibit Ca_V channels is important for perspectives on their (patho) physiological roles and could advance their development and use as genetically-encoded Ca_V channel blockers. We previously reported that Rem can block surface $Ca_V1.2$ channels in 2 independent ways that engage distinct components of the channel complex: (1) by binding auxiliary β subunits (β-binding-dependent inhibition, or BBD); and (2) by binding the pore-forming α_{1C} subunit N-terminus (α_{1C}-binding-dependent inhibition, or ABD). By contrast, Gem uses only the BBD mechanism to block $Ca_V1.2$. Rem molecular determinants required for BBD $Ca_V1.2$ inhibition are the distal C-terminus and the guanine nucleotide binding G-domain which interact with the plasma membrane and $Ca_V\beta$, respectively. However, Rem determinants for ABD $Ca_V1.2$ inhibition are unknown. Here, combining fluorescence resonance energy transfer, electrophysiology, systematic truncations, and Rem/Gem chimeras we found that the same Rem distal C-terminus and G-domain also mediate ABD $Ca_V1.2$ inhibition, but with different interaction partners. Rem distal C-terminus interacts with α_{1C} N-terminus to anchor the G-domain which likely interacts with an as-yet-unidentified site. In contrast to some previous studies, neither the C-terminus of Rem nor Gem was sufficient to inhibit Ca_V1/Ca_V2 channels. The results reveal that similar molecular determinants on Rem are repurposed to initiate 2 independent mechanisms of $Ca_V1.2$ inhibition.

ARTICLE HISTORY
Received 12 April 2016
Accepted 13 April 2016

KEYWORDS
CaV1.2; L-type calcium channel; Gem; Rem; RGK protein

Introduction

High-voltage-activated (HVA) calcium channels ($Ca_V1.1$–1.4, $Ca_V2.1$–2.3) couple electrical excitation to physiological responses in excitable cells.[1] These channels are hetero-oligomeric protein complexes comprising a pore-forming α_1-subunit assembled with auxiliary proteins that include $\beta/\alpha_2\delta/\gamma$ subunits and calmodulin.[2,3] There are 7 genes coding for HVA calcium channel α_1-subunits, each with multiple splice variants. The transmembrane α_1-subunit defines the channel subtype and contains the voltage sensor, the selectivity filter, and the water-filled pore that provides a passageway for Ca^{2+} ions to traverse the hydrophobic plasma membrane. The auxiliary subunits profoundly regulate the trafficking and gating properties of α_1-subunits and are essential for the physiological function of Ca_V1/Ca_V2 channels. In particular, $Ca_V\beta$ (β_1-β_4) is crucial for forming functional Ca_V1/Ca_V2 channels as it is obligatory for α_1 trafficking to the cell surface, increases the open probability (P_O) of surface channels, and imposes isoform-dependent inactivation gating signatures.[4,5] Modulation of specific Ca_V1/Ca_V2 channels by signaling proteins, Ca^{2+} ions, or small molecules is a powerful method to regulate diverse aspects of physiology including cardiac contractility, synaptic plasticity, insulin release, and gene expression.[2,6-9] Molecules that block Ca_V1/Ca_V2 channels with high specificity and potency are sought after as therapeutics for various cardiovascular and neurological disorders including cardiac arrhythmias, pain, and neurodegenerative diseases.[10-12]

CONTACT Henry M. Colecraft, PhD hc2405@columbia.edu Department of Physiology and Cellular Biophysics, Columbia University, College of Physicians and Surgeons, 1150 St. Nicholas Avenue, 504 Russ Berrie, New York, NY 10032, USA.

Color versions of one or more of the figures in the article can be found online at www.tandfonline.com/kchl.

Supplemental data for this article can be accessed on the publisher's website.

Rad, Rem, Rem2 and Gem/Kir (RGK) proteins are Ras-like monomeric G-proteins that potently and non-selectively inhibit all Ca_V1/Ca_V2 channels.[13-16] Distinct RGK proteins are expressed in muscle, neurons, pancreas, and immune cells, and knockout mice studies suggest their inhibition of Ca_V channels is physiologically relevant in different systems.[17-22] The potential of using RGK proteins as precisely targeted genetically-encoded Ca_V channel blockers for therapeutic applications has been explored in proof-of-concept experiments in heart *in vivo* and *in vitro*.[23,24] A major limitation to the practical use of RGKs as Ca_V channel blockers is that they non-selectively inhibit Ca_V1/Ca_V2 channels. Development of selective RGK-derived Ca_V1/Ca_V2 channel inhibitors could accelerate their applied use as genetically-encoded Ca_V channel blockers.

All four RGK proteins interact directly with $Ca_V\beta$.[13,14,25] Recently, we examined the role of Rem/$Ca_V\beta$ interaction in Rem inhibition of recombinant $Ca_V1.2$ channels using a mutant β_{2a} (β_{2aTM}) which contains point mutations (D243A, D319A and D321A) that selectively abolish binding to RGK proteins,[25] but retains the capacity to modulate Ca_V1/Ca_V2 channel trafficking and gating.[26] We discovered that Rem utilizes 2 independent pathways to inhibit $Ca_V1.2$ channels—a β-binding-dependent (BBD) mode and a direct α_{1C}-binding-dependent (ABD) mechanism, respectively. The BBD pathway likely explains the indiscriminate nature of RGK inhibition since all Ca_V1/Ca_V2 channels require assembly with β for their functional maturation.[4,5] Understanding the molecular bases for the ABD Rem inhibition of $Ca_V1.2$ is of special interest because this mechanism could potentially be exploited to develop Ca_V1/Ca_V2 isoform-selective channel blockers. The ABD mechanism of $Ca_V1.2$ inhibition requires Rem binding to α_{1C} N-terminus (α_{1C}NT).[26] However, the determinants on Rem itself necessary for binding α_{1C}NT and initiating ABD $Ca_V1.2$ inhibition are unknown. Here, we report that the Rem distal C-terminus (Rem_{DCT}) and guanine nucleotide binding domain (G-domain) are both required for ABD $Ca_V1.2$ inhibition. Rem_{DCT} binds α_{1C}NT anchoring the G-domain, which presumably engages with an as-yet-unidentified site either within the channel complex or elsewhere, to initiate $Ca_V1.2$ inhibition. Remarkably, these same Rem determinants—Rem_{DCT} and G-domain—are also utilized, but with different interaction partners (plasma membrane and $Ca_V\beta$, respectively), for BBD $Ca_V1.2$ inhibition.[26-29]

Results

Rem and Gem differ in their capacity to use an α_{1C}-binding-dependent mechanism to inhibit $Ca_V1.2$ channels

It is now well-established that RGK proteins strongly inhibit currents through Ca_V1/Ca_V2 channels.[13-16,30-33] Here, we recapitulate this effect by examining the impact of Rem and Gem on $Ca_V1.2$ channels reconstituted by transient transfection of HEK293 cells with $\alpha_{1C} + \beta_{2a}$ subunits. As expected, control cells express large whole-cell L-type currents ($I_{Ca,L}$) which are deeply inhibited equally by either co-expressed Rem or Gem (Fig. 1A, B). To isolate the ABD component underlying RGK inhibition of $I_{Ca,L}$, we reconstituted $Ca_V1.2$ with a β_{2a} triple mutant (β_{2aTM}) that does not bind RGKs but retains modulatory actions on the channel complex.[25,26] Channels reconstituted with $\alpha_{1C} + \beta_{2aTM}$ display robust currents which are differentially affected by Rem and Gem, respectively. Whereas Rem significantly inhibits $\alpha_{1C} + \beta_{2aTM}$ channels, Gem has no impact on $I_{Ca,L}$ through these mutant $Ca_V1.2$ channels (Fig. 1C,D). These results confirm our recent finding that Gem uses a solely BBD mechanism to inhibit $Ca_V1.2$ channels, whereas Rem uses both BBD and ABD pathways to achieve $I_{Ca,L}$ block.[26]

α_{1C}-binding-dependent Rem inhibition of $I_{Ca,L}$ occurs in cardiac myocytes

The molecular determinants and mechanisms that distinct RGK proteins use to inhibit Ca_V channels can differ substantively in different cell types.[30-32,34,35] Whether Rem inhibits endogenous $Ca_V1.2$ channels in their native context using the ABD mechanism is unknown. This information is crucial to gauge the potential physiological significance of this mode of channel inhibition and whether it can be exploited to design generally useful Ca_V1/Ca_V2 isoform-selective inhibitors. We previously showed that over-expressing an α_{1C}NT peptide eliminates ABD $Ca_V1.2$ inhibition by competitively interfering with Rem binding to the full-length α_{1C} N-terminus.[26] We exploited this approach to determine whether Rem inhibits endogenous $Ca_V1.2$ channels in cardiac myocytes using the ABD mechanism.

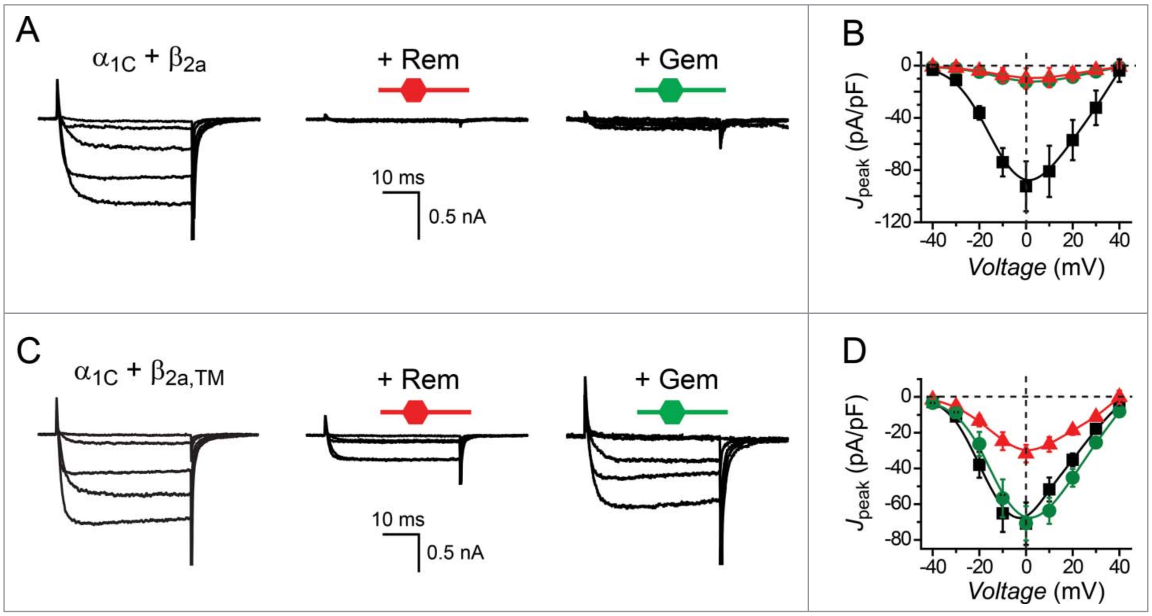

Figure 1. Rem and Gem differ in their capacity to use a α_{1C}-binding-dependent mechanism to inhibit $Ca_V1.2$ channels. (A) Exemplar Ba^{2+} currents from HEK293 cells expressing wild-type $Ca_V1.2$ ($\alpha_{1C} + \beta_{2a}$) (*left*) in the presence of either Rem (*middle*) or Gem (*right*). (B) Population current density (J_{peak}) vs. voltage relationships for wild-type $Ca_V1.2$ channels (■, $n = 6$) co-expressed with either Rem (▲, $n = 3$) or Gem (●, $n = 4$). (C) Exemplar Ba^{2+} currents from HEK293 cells expressing mutant $Ca_V1.2$ ($\alpha_{1C} + \beta_{2aTM}$) (*left*) in the presence of either Rem (*middle*) or Gem (*right*). (D) J_{peak}—*voltage* relationships for mutant $Ca_V1.2$ channels (■, $n = 9$) co-expressed with Rem (▲, $n = 7$) or Gem (●, $n = 8$). Data are means ± SEM.

Whole-cell patch clamp of cultured adult rat ventricular myocytes yielded large Ba^{2+} currents (Fig. 2, A and B; $I_{peak} = -15.5 \pm 1.6$ pA/pF, $n = 8$). Adenoviral-mediated over-expression of Rem-IRES-mCherry dramatically inhibited whole-cell current (Fig. 2, C and D; $I_{peak} = -1.2 \pm 0.2$ pA/pF, $n = 8$; $P < 0.05$ compared to control). Co-expressing CFP-α_{1C}NT together with Rem-IRES-mCherry resulted in a partial rescue of current (Fig. 2, E and F; $I_{peak} = -5.6 \pm 1.2$ pA/pF, $n = 8$; $P < 0.05$ compared to Rem-IRES-mCherry alone), consistent with a

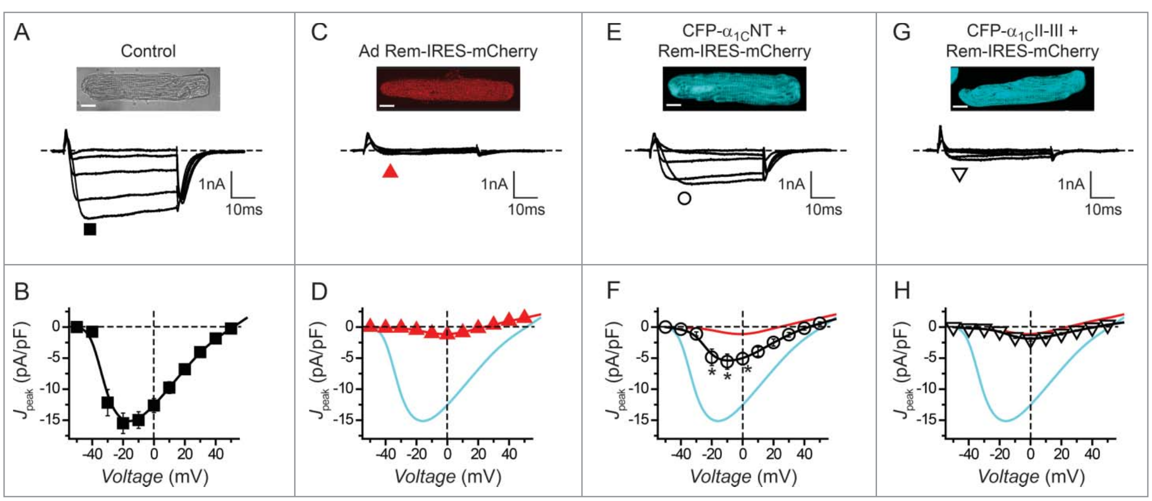

Figure 2. Cardiac myocytes possess a β-binding-independent mechanism to inhibit endogenous $Ca_V1.2$ channels. (A) *Top*, Gray scale image of rat ventricular myocyte. Scale bar, 10 μm. *Bottom*, representative whole-cell $Ca_V1.2$ channel currents from a cultured rat ventricular myocyte expressing CFP-α_{1C}NT (■, $n = 8$). (B) Population J_{peak}—V relationship for control cardiomyocytes. (C-H) Data for cardiomyocytes expressing Rem-IRES-mCherry (▲, $n = 8$), CFP-α_{1C}NT + Rem-IRES-mCherry (O, $n = 10$) and CFP-α_{1C}II-III loop + Rem-IRES-mCherry (▽, $n = 8$), respectively; same format as A and B. Data for control (cyan line) and Rem-IRES-mCherry (red line) are reproduced for comparison. * $P < 0.05$ compared to either Rem-IRES-mCherry or control, one-way ANOVA.

significant contribution of the ABD mechanism to Rem inhibition of $Ca_V1.2$ in cardiac myocytes. This result was not due to the potentially trivial explanation that co-infecting myocytes with 2 adenoviruses led to reduced Rem expression because co-expressing CFP-α_{1C} II-III loop did not appreciably rescue current blocked by Rem-IRES-mCherry (Fig. 2, G and H; $I_{peak} = -1.9 \pm 0.3$ pA/pF, $n = 8$). Patched cells were monitored for CFP and mCherry fluorescence ensuring that both proteins were expressed in the selected cardiomyocytes (Fig. S1).

These results demonstrate that ABD Rem inhibition of $Ca_V1.2$ occurs in a physiological context and provided strong motivation to probe the Rem molecular determinants underlying this mode of $Ca_V1.2$ inhibition.

Rem distal C-terminus interacts with α_{1C}NT

How does Rem interact with α_{1C}NT, and are the determinants for this interaction lacking in Gem? Initial expectations for answers to these questions were derived from comparing Rem and Gem primary sequences. Mouse Rem contains 297 amino acids and can be nominally divided into 3 parts based on comparison with the prototypical Ras: N-terminus (residues 1–77), G-domain (residues 78–246), and C-terminus (residues 247–297) (Fig. 3). Ras is principally composed of a G-domain, a structure comprised of a 6-stranded β-sheet surrounded by 5 α-helices with 5 conserved loops (G1-G5) that form the guanine-nucleotide binding site.[36,37] The G-domains of all 4 RGK proteins are highly conserved, bind guanine nucleotides, and adopt a similar structural fold as the Ras G-domain.[15,38] The N-terminus extensions of Rem and Gem are variable (< 30% homology); the C-termini extensions contain a variable proximal region (PCT; residues 247–257 in Rem and 244–256 in Gem, respectively) and a conserved distal region (DCT; 70% homology) (Fig. 3).

We used a 3-cube fluorescence resonance energy transfer (FRET) assay[39-41] to determine which regions of Rem associate with α_{1C}NT and how these compared with determinants required for binding $Ca_V\beta$ (Fig. 4) We generated YFP-α_{1C}NT and YFP-β_3, respectively, and used these in 3-cube FRET experiments with CFP-tagged wild-type (wt) Rem and Rem-deletion mutants, respectively. As a negative control for these experiments, we first measured FRET between CFP-FRB and either YFP-α_{1C}NT or YFP-β_3, respectively. FRB is the rapamycin-binding domain from the kinase mTor,[42,43] and is not expected to associate with either YFP-α_{1C}NT or YFP-β_3. HEK293 cells co-expressing CFP-FRB and either YFP-α_{1C}NT or YFP-β_3 displayed low FRET efficiencies ($FRET_{eff}$) of 0.018 ± 0.005 and 0.031 ± 0.004, respectively (Fig. 4, B and C). By contrast, cells expressing CFP-Rem and either YFP-α_{1C}NT or YFP-β_3 displayed significantly elevated $FRET_{eff}$ of 0.147 ± 0.011 ($n = 37$) and 0.150 ± 0.007 ($n = 42$), respectively (Fig. 4, B and C). A

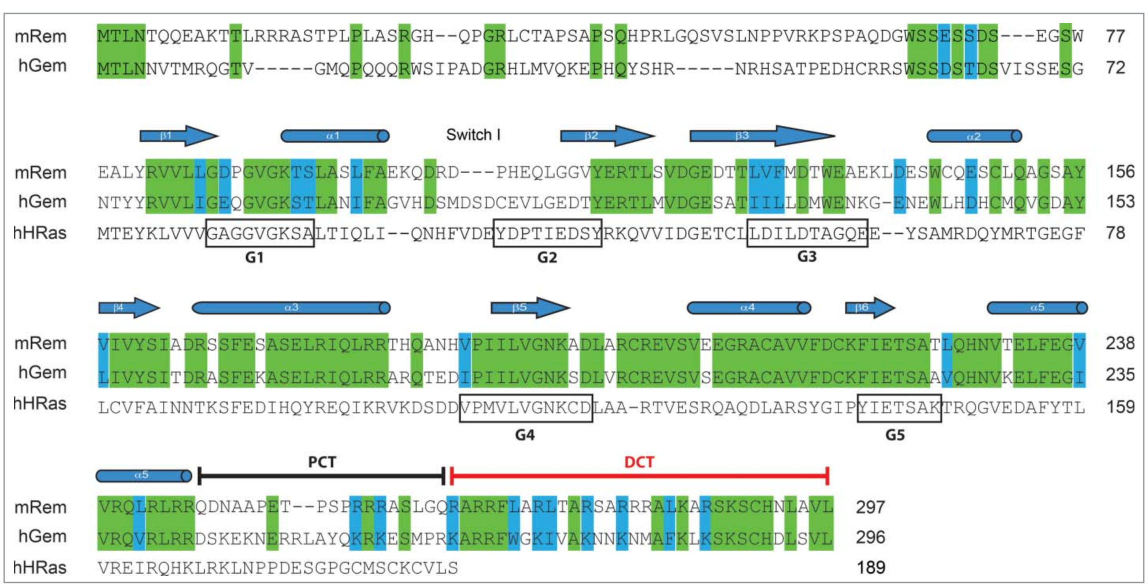

Figure 3. Primary sequence alignment of Rem and Gem. Sequence alignment of murine Rem, human Gem and human H-Ras. Identical residues are shaded green; similar residues are shaded in cyan. PCT, proximal C-terminus; DCT, distal C-terminus.

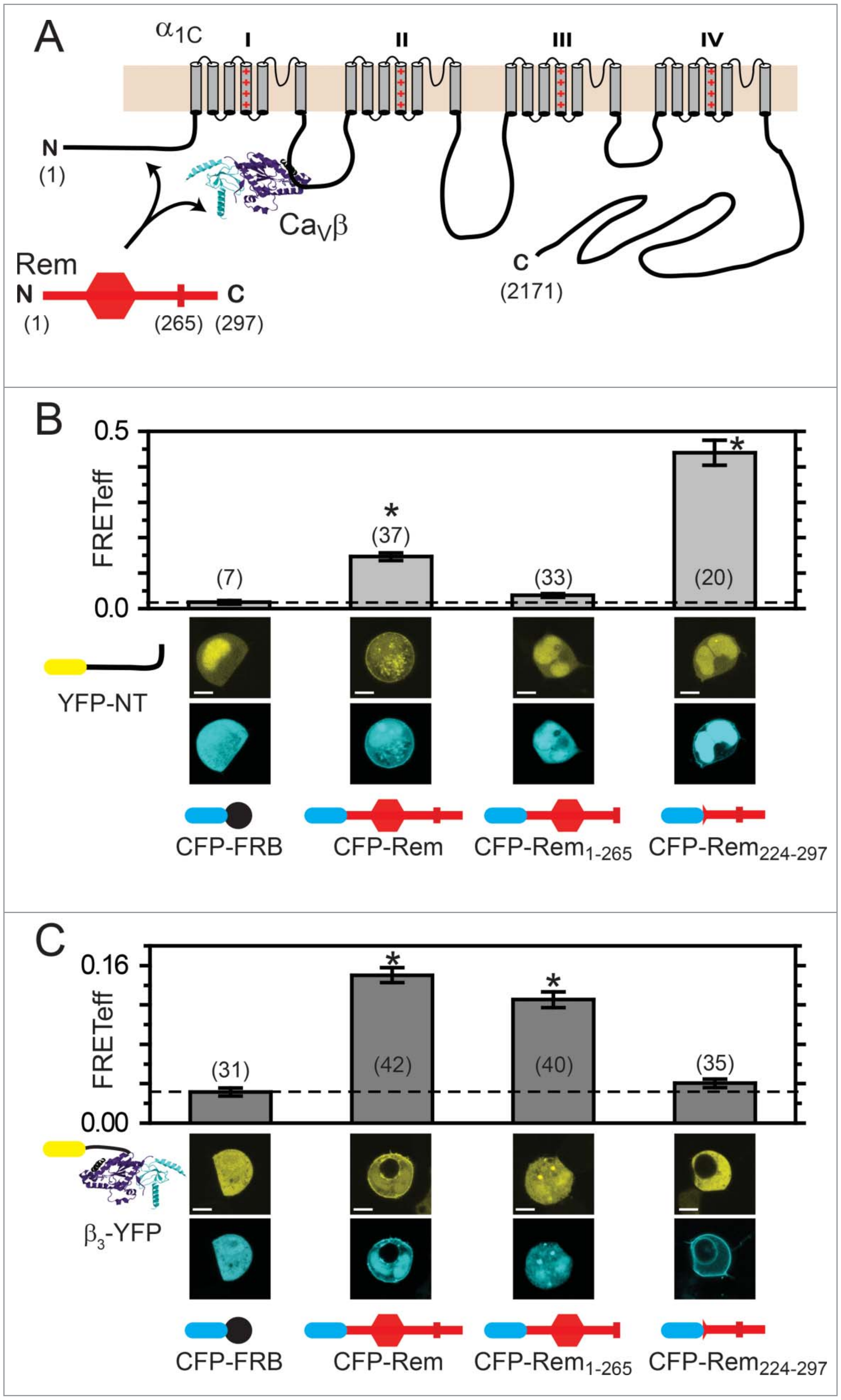

Figure 4. FRET detection of Rem determinants underlying interaction with α_{1C} N-terminus and $Ca_V\beta$. (A) Schematic of α_{1C}, $Ca_V\beta$, and Rem. Rem interacts independently with $Ca_V\beta$ and α_{1C} N-terminus. (B) FRET detection of interactions between YFP-α_{1C}NT and distinct CFP-tagged wt or truncated Rem constructs. $^*P < 0.05$ compared with CFP-FRB using one-way ANOVA and Bonferroni test (C) FRET detection of interactions between YFP-$Ca_V\beta_3$ and distinct CFP-tagged wt or truncated Rem constructs. $^*P < 0.05$ compared with CFP-FRB using one-way ANOVA and Bonferroni test. Data are means $\pm$ SEM.

truncated Rem lacking the final 32 amino acids of the C-terminus (CFP-Rem$_{1-265}$) displayed no interaction with YFP-α_{1C}NT (FRET$_{eff}$ = 0.037 ± 0.005, n = 33) (Fig. 4B), while the association with YFP-β_3 was preserved (FRET$_{eff}$ = 0.125 ± 0.008, n = 40) (Fig. 4C). Conversely, CFP-Rem$_{224-297}$ which lacks the Rem N-terminus and most of the G-domain showed robust binding to YFP-α_{1C}NT (FRET$_{eff}$ = 0.439 ± 0.035, n = 20) but no interaction with YFP-β_3 (FRET$_{eff}$ = 0.040 ± 0.004, n = 35) (Fig. 4, B and C). Consistent with these results, YFP-Rem, but not YFP-Rem$_{265}$, interacted with full-length CFP-α_{1C} as reported by an elevated FRET efficiency (Fig. S2).

Taken together with previous results, these data support the binary interpretation that separate determinants underlie Rem binding to α_{1C}NT and Ca$_V\beta$, respectively: the Rem$_{DCT}$ is responsible for association with α_{1C}NT but plays no role in binding Ca$_V\beta$; Rem G-domain mediates interaction with Ca$_V\beta$ but does not contribute to α_{1C}NT binding.

Rem$_{DCT}$ determinants required for binding α_{1C}NT and ABD Ca$_V$1.2 inhibition

To more precisely localize the residues within Rem$_{DCT}$ responsible for binding α_{1C}NT we generated 2 additional Rem deletion mutants (CFP-Rem$_{1-285}$ and CFP-Rem$_{1-275}$) and used FRET to assess their interaction with YFP-α_{1C}NT (Fig. 5). CFP-Rem$_{1-285}$ co-expressed with YFP-α_{1C}NT yielded a robust FRET signal (FRET$_{eff}$ = 0.071 ± 0.01, n = 32) that was comparable to that obtained with wt CFP-Rem (FRET$_{eff}$ = 0.085 ± 0.009, n = 24, P = 1 compared to CFP-Rem$_{1-285}$) (Fig. 5B). By contrast, CFP-Rem$_{1-275}$ displayed a significantly reduced FRET signal when co-expressed with YFP-α_{1C}NT (FRET$_{eff}$ = 0.040 ± 0.009, n = 13, P = 0.028 compared to CFP-Rem, one-way ANOVA), consistent with reduced binding between the 2 proteins (Fig. 5B). These results were bolstered by complementary co-immunoprecipitation experiments (Fig. 5C). We co-expressed CFP-tagged wt Rem or the deletion mutants without (lane 1) or with (lanes 2–5) YFP-α_{1C}NT in HEK293 cells. Western blots of whole-cell lysates using anti-GFP antibody showed similar expression levels of all the Rem constructs, and confirmed the presence of co-expressed YFP-α_{1C}NT (Fig. 5C, *top*). Immunoprecipitation using anti-Rem antibody led to comparable pull-down of all the Rem constructs. However, the amount of YFP-α_{1C}NT that was co-immunoprecipitated differed among the various groups. A comparable amount of YFP-α_{1C}NT was pulled down with CFP-Rem and CFP-Rem$_{1-285}$, respectively. By comparison, a substantially lower quantity of YFP-α_{1C}NT was co-immunoprecipitated with CFP-Rem$_{1-275}$ and CFP-Rem$_{1-265}$, respectively.

We next comparatively evaluated how effectively the distinct Rem C-terminus deletion mutants inhibited Ca$_V$1.2 channels using the BBD and ABD mechanisms, respectively. Cells expressing either wt (α_{1C}/β_{2a}) or mutant (α_{1C}/β_{2aTM}) Ca$_V$1.2 channels were both inhibited by wt Rem but unaffected by Rem$_{1-265}$, indicating that both the BBD and ABD mechanisms require Rem$_{DCT}$ (Fig. 5D). Rem$_{1-285}$ inhibited both α_{1C}/β_{2a} and α_{1C}/β_{2aTM} channels with a pattern indicating that both the BBD and ABD pathways were largely intact (Fig. 5D). By contrast, Rem$_{1-275}$ significantly inhibited α_{1C}/β_{2a} but not α_{1C}/β_{2aTM} channels (Fig. 5D), indicating a selective loss of the ABD mode of inhibition. These data show that both the BBD and ABD modes of inhibition require Rem$_{DCT}$ but not in an identical manner.

Rem C-terminus is not sufficient to inhibit Ca$_V$1.2

Could the interaction between Rem C-terminus and α_{1C} be sufficient to inhibit Ca$_V$1.2? We explored this question by assessing the impact of a construct containing the last 75 amino acids of Rem (CFP-Rem$_{224-297}$) on $I_{Ca,L}$ from HEK293 cells expressing either wt (α_{1C}/β_{2a}) or mutant (α_{1C}/β_{2aTM}) Ca$_V$1.2 channels (Fig. 6). A similar extended C-terminus construct derived from Gem was previously reported to be sufficient to inhibit recombinant Ca$_V$2.1 channels.[44] Surprisingly, CFP-Rem$_{224-297}$ had no effect on either α_{1C}/β_{2a} or α_{1C}/β_{2aTM} channels (Fig. 6, A and B), indicating Rem C-terminus is necessary but not sufficient for either BBD or ABD Ca$_V$1.2 inhibition. This result implied an additional structural component in Rem is required for the observed ABD inhibition of Ca$_V$1.2.

Rem G-domain is required for ABD Ca$_V$1.2 inhibition

We used a chimeric method to probe which additional Rem structural component(s) is required for BBD Ca$_V$1.2 inhibition. The approach exploited the functional difference between Rem and Gem with regards to the prevalence of the 2 distinct modes of Ca$_V$1.2 inhibition: whereas Rem diminishes $I_{Ca,L}$ using both

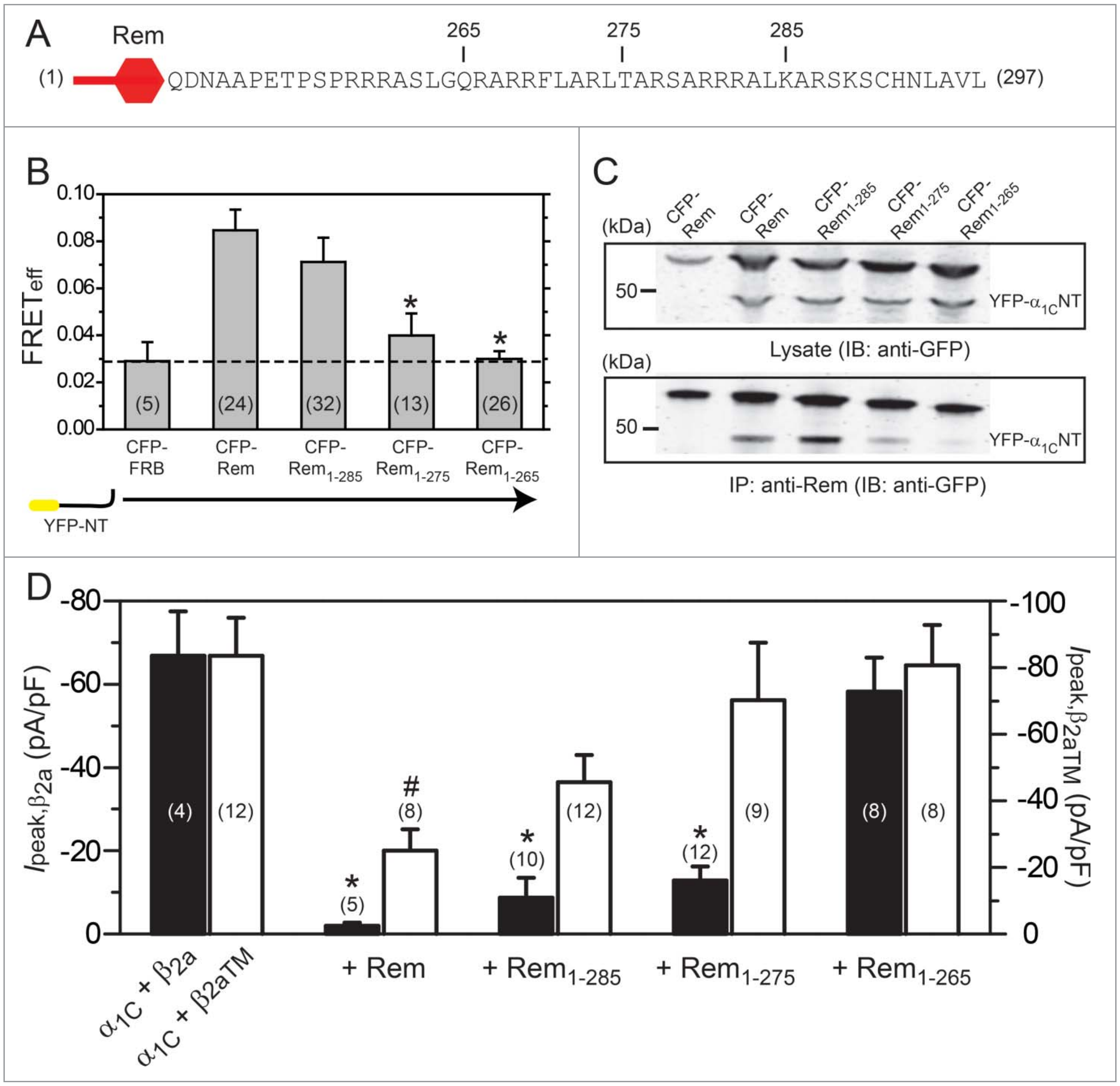

Figure 5. Mapping Rem distal C-terminus determinants required for β-binding-dependent and α_{1C}-binding-dependent inhibition of $Ca_V1.2$ (A) Sequence of Rem C-terminus with truncation sites indicated for Rem_{1-265}, Rem_{1-275}, and Rem_{1-285}. (B) FRET detection of interactions between YFP-α_{1C}NT and distinct CFP-tagged wt or truncated Rem constructs. $^*P < 0.05$ compared with CFP-Rem using one-way ANOVA and Bonferroni test. Data are means ± SEM (C) Co-immunoprecipitation detection of interactions between YFP-α_{1C}NT and CFP-tagged wt or truncated Rem constructs. Top panel shows Western blot of whole-cell lysates (input). (D) Bar chart showing mean peak current density from wild-type (black) and mutant (white) $Ca_V1.2$ channels ± wt or truncated Rem constructs. #$P < 0.05$ compared with $\alpha_{1C} + \beta_{2a}$ using one-way ANOVA and Bonferroni tests. $^*P < 0.05$ compared with $\alpha_{1C} + \beta_{2aTM}$ using one-way ANOVA and Bonferroni tests. Data are means ± SEM.

BBD and ABD mechanisms, Gem utilizes only the BBD pathway (Fig. 1). The inability of Gem to reconstitute ABD $Ca_V1.2$ inhibition could be due to a failure to bind α_{1C}-NT. Alternatively, Gem could potentially bind α_{1C}-NT well but lack the additional component required to transduce the functional effect. FRET experiments in cells co-expressing CFP-Gem and YFP-α_{1C}NT indicated no interaction between the 2 proteins (Fig. 7A). Could simply donating the capacity to bind α_{1C}-NT to Gem be sufficient to reconstitute ABD $Ca_V1.2$ block? To address this we examined the functional properties of a chimeric protein, Gem-r, in which the C-terminus of Gem was replaced with the corresponding region from Rem. Cells co-expressing YFP-α_{1C}NT and CFP-Gem-r displayed robust FRET indicating successful transplantation of the capacity to directly bind α_{1C} (Fig. 7A). Functionally, CFP-Gem-r potently inhibits wt α_{1C}/β_{2a} but has no effect on $I_{Ca,L}$ recorded from mutant α_{1C}/β_{2aTM} channels (Fig. 7B), indicating this chimera displays only BBD $Ca_V1.2$

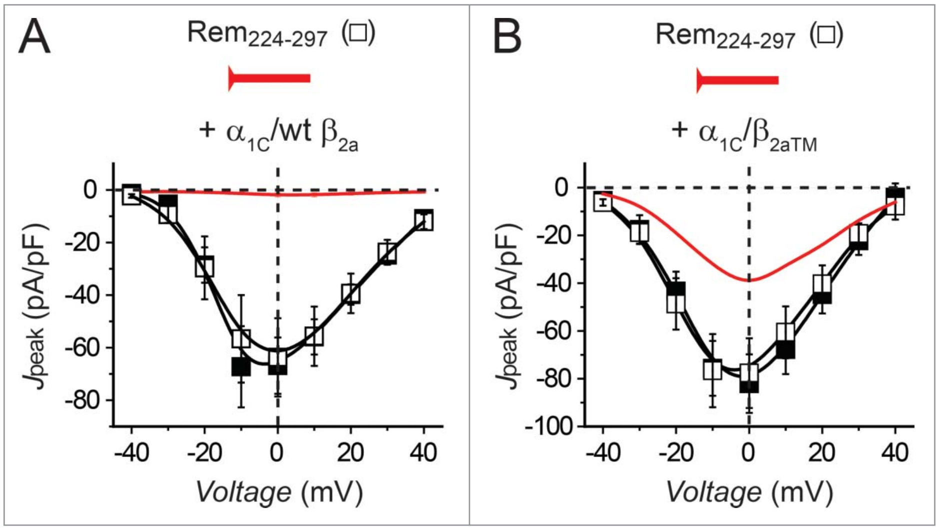

Figure 6. Rem C-terminus is not sufficient for $Ca_V1.2$ inhibition. (A) J_{peak}–V relationships for $\alpha_{1C} + \beta_{2a}$ (■, $n = 4$) and $\alpha_{1C} + \beta_{2a} + Rem_{224-297}$ ($n = 8$) channels. (B) J_{peak}–V relationships for $\alpha_{1C} + \beta_{2aTM}$ (■, $n = 9$) and $\alpha_{1C} + \beta_{2aTM} + Rem_{224-297}$ (□, $n = 6$) channels.

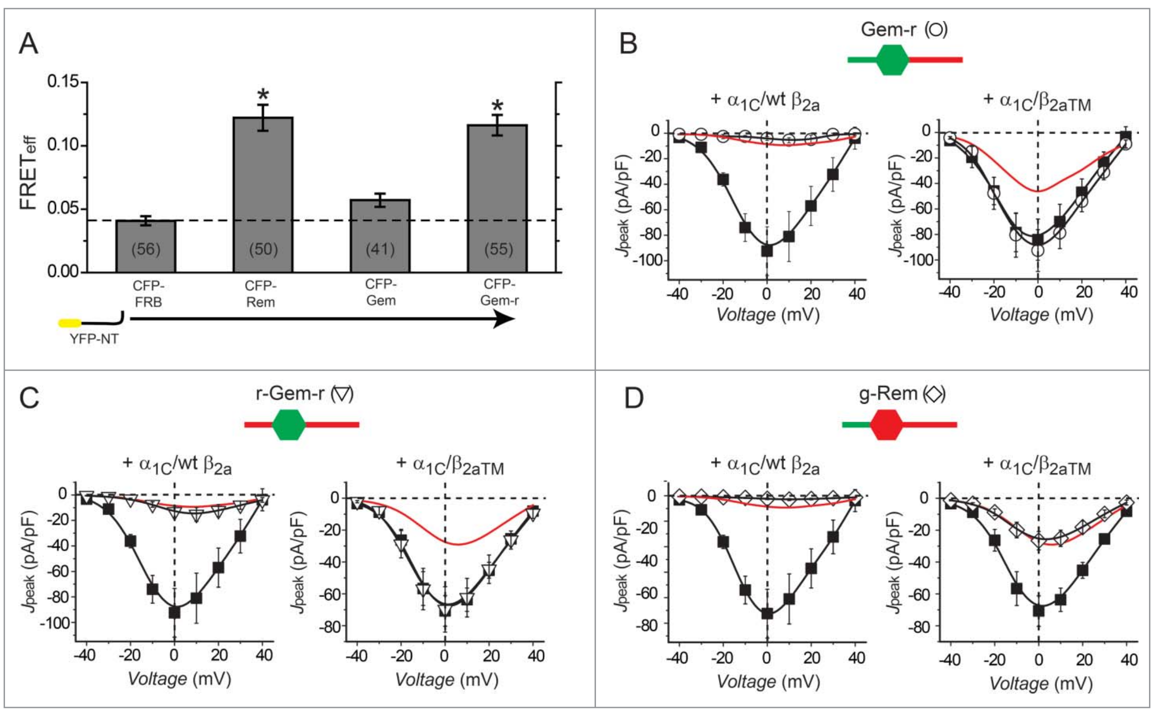

Figure 7. Chimeric Rem/Gem analyses of determinants required for α_{1C}-binding-dependent $Ca_V1.2$ inhibition. (A) FRET detection of interactions between YFP-α_{1C}NT and CFP-tagged Rem/Gem constructs. $^*P < 0.05$ compared with CFP-FRB using one-way ANOVA and Bonferroni tests. Data are means ± SEM. (B) *Left*, J_{peak}–V relationships for $\alpha_{1C} + \beta_{2a}$ (■, $n = 6$) and $\alpha_{1C} + \beta_{2a}$ + Gem-r (O, $n = 4$) channels. Data for $\alpha_{1C} + \beta_{2a}$ + Rem is reproduced for comparison (red line). *Right*, J_{peak}–V relationships for $\alpha_{1C} + \beta_{2aTM}$ (■, $n = 9$) and $\alpha_{1C} + \beta_{2aTM}$ + Gem-r (O, $n = 8$) channels. Data for $\alpha_{1C} + \beta_{2aTM}$ + Rem is reproduced for comparison (red line). (C) *Left*, J_{peak}–V relationships for $\alpha_{1C} + \beta_{2a}$ (■, $n = 6$) (data are same as in (B)) and $\alpha_{1C} + \beta_{2a}$ + r-Gem-r (▽, $n = 7$) channels. Data for $\alpha_{1C} + \beta_{2a}$ + Rem is reproduced for comparison (red line). *Right*, J_{peak}–V relationships for $\alpha_{1C} + \beta_{2aTM}$ (■, $n = 9$) and $\alpha_{1C} + \beta_{2aTM}$ + r-Gem-r (▽, $n = 10$) channels. Data for $\alpha_{1C} + \beta_{2aTM}$ + Rem is reproduced for comparison (red line). (D) *Left*, J_{peak}–V relationships for $\alpha_{1C} + \beta_{2a}$ (■, $n = 6$) (data are same as in (B)) and $\alpha_{1C} + \beta_{2a}$ + g-Rem (◊, $n = 9$) channels. Data for $\alpha_{1C} + \beta_{2a}$ + Rem is reproduced for comparison (red line). *Right*, J_{peak}–V relationships for $\alpha_{1C} + \beta_{2aTM}$ (■, $n = 9$) (data are same as in (C)) and $\alpha_{1C} + \beta_{2aTM}$ + g-Rem (◊, $n = 8$) channels. Data for $\alpha_{1C} + \beta_{2aTM}$ + Rem is reproduced for comparison (red line). Data are means ± SEM.

inhibition. Hence, simply targeting Gem to α_{1C}-NT is not sufficient to reconstitute ABD inhibition of $Ca_V1.2$. The results further suggested that additional component(s) present in Rem N-terminus and/or G-domain but lacking in Gem were necessary for ABD inhibition of $Ca_V1.2$.

We generated 2 additional chimeras to test this assumption: r-Gem-r contains the N- and C-terminus extensions of Rem appended to Gem G-domain; and g-Rem which consists of Gem N-terminus attached to Rem G-domain and C-terminus. Both r-Gem-r and g-Rem retained the capacity to potently inhibit wt α_{1C}/β_{2a} channels (Fig. 7, C and D). By contrast, the 2 chimeras showed a sharp dichotomy in their impact on mutant α_{1C}/β_{2aTM} channels—r-Gem-r was without effect while g-Rem inhibited these channels to the same extent as wt Rem. Taken together, the results indicate that the ABD mode of $Ca_V1.2$ inhibition minimally requires both the Rem_{DCT} and G-domain.

Discussion

This study provides new insights into molecular determinants underlying Rem-mediated inhibition of $Ca_V1.2$ channels. The data demonstrate that Rem_{DCT} binds α_{1C}NT to initiate ABD Rem inhibition of $Ca_V1.2$ channels. However, Rem C-terminus is not by itself sufficient to reconstitute ABD inhibition. Chimeric Rem/Gem analyses indicated that Rem (but not Gem) G-domain is also necessary for the ABD mechanism of $Ca_V1.2$ inhibition.

The finding that Rem_{DCT} and G-domain are the essential motifs required for ABD inhibition of $Ca_V1.2$ was unexpected for 2 main reasons. First, previous work has established that these same 2 regions also underlie BBD Rem inhibition of $Ca_V1.2$.[26-29,32] To activate BBD inhibition, Rem_{DCT} binds the plasma membrane while the G-domain interacts with $Ca_V\beta$ in the channel complex. This configuration essentially uses Rem to cross-link $Ca_V\beta$ and by association, the intracellular α_{1C} I-II loop, to the plasma membrane (Fig. 8). This is hypothesized to induce a conformational change that effectively closes the channel pore. We previously exploited these insights into the BBD inhibition mechanism to develop a general approach— termed channel inactivation induced by membrane-tethering an associated protein (ChIMP)—for generating novel genetically-encoded Ca_V1/Ca_V2 channel blockers.[27] For the ABD inhibition pathway, this study shows that Rem_{DCT} and G-domain are also utilized, but do so by interacting with different binding partners. In this case, Rem_{DCT} interacts with α_{1C}NT. Precisely how the Rem G-domain participates in ABD inhibition of $Ca_V1.2$ is not clear. We can deduce it plays an active role in the process because the homologous Gem G-domain cannot substitute for its function. The most likely scenario is that Rem G-domain selectively binds to another site within the cell, effectively cross-linking α_{1C}NT to an intracellular anchor to initiate ABD $Ca_V1.2$ inhibition (Fig. 8). Candidate regions for the putative Rem G-domain interaction site include somewhere on the α_{1C} subunit itself or the cytoskeleton. RGK proteins are known to interact with and regulate the cytoskeleton.[15,45] Identification of the presumed interaction site for Rem G-domain that is necessary for ABD $Ca_V1.2$ inhibition is an important goal for future studies.

The second reason why the finding that Rem_{DCT} and G-domain underlie ABD inhibition was surprising is that these 2 regions are the most highly conserved among RGK proteins. Nevertheless, Gem and Rem2 lack the capacity for ABD $Ca_V1.2$ inhibition.[26] The distal C-termini of all 4 RGKs anchor the respective proteins to the plasma membrane.[46] Similarly, the G-domains of all RGKs bind $Ca_V\beta$. The dual capability of all RGKs to bind the plasma membrane and $Ca_V\beta$s provides a simple explanation for the rather unique feature that RGKs potently and non-selectively inhibit *all* Ca_V1/Ca_V2 channels, *i.e.* they accomplish this through the BBD pathway. The unique capability of Rem to bind α_{1C}NT and initiate ABD $Ca_V1.2$ inhibition reveals functional specialization among RGK C-termini and G-domains despite their high sequence homology.

Deepened understanding of how ABD inhibition arises could potentially be exploited to design novel genetically-encoded Ca_V channel blockers, in the same manner as we previously accomplished with the BBD mode of inhibition.[27] The particular advantage of leveraging the ABD pathway in this manner is the likelihood that this approach could yield *isoform-selective* genetically-encoded Ca_V1/Ca_V2 blockers. One potential merit of such blockers is that they can be genetically targeted to precise cell populations and

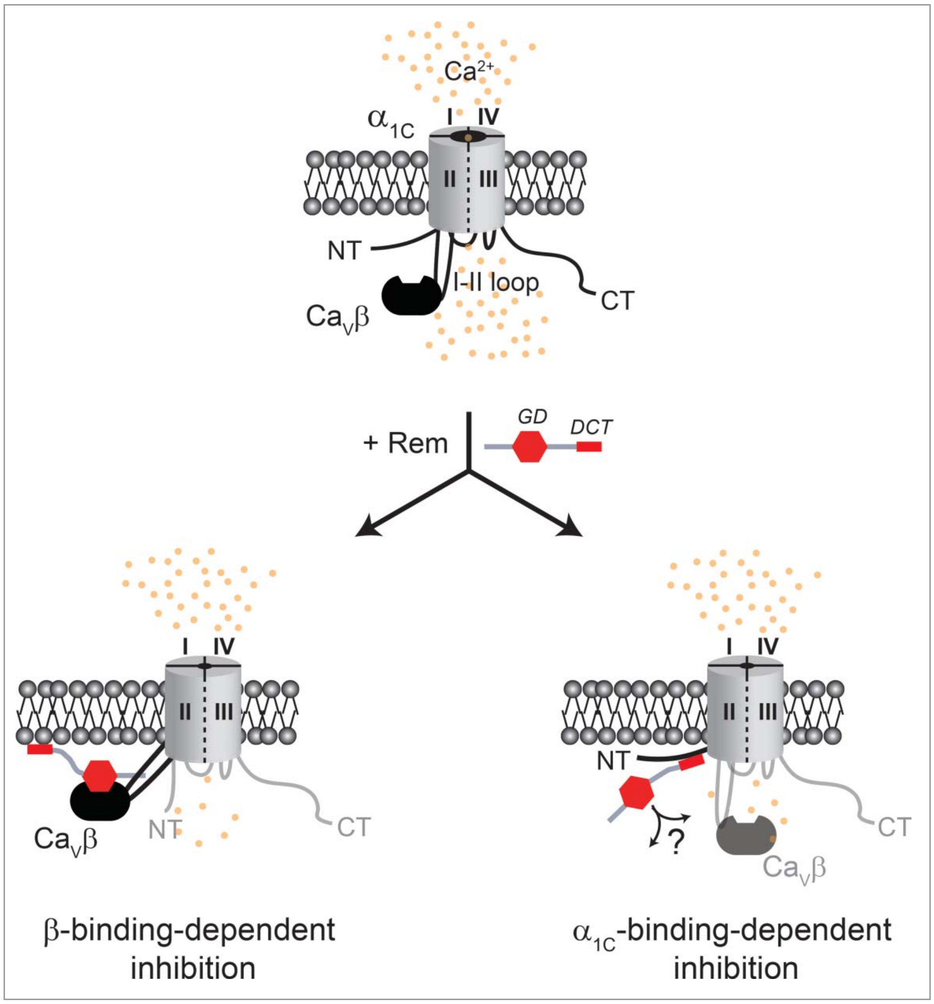

Figure 8. Rem distal C-terminus and G-domain underlie both β-binding-dependent and α_{1C}-binding-dependent $Ca_V1.2$ inhibition. Cartoon showing Rem determinants and putative interaction sites responsible for β-binding-dependent and α_{1C}-binding-dependent $Ca_V1.2$ inhibition. Both types of inhibition rely on the Rem distal C-terminus (DCT) and G-domain (GD). For β-binding-dependent inhibition, Rem_{DCT} and GD bind the plasma membrane and $Ca_V\beta$, respectively. For α_{1C}-binding-dependent inhibition Rem_{DCT} binds α_{1C} N-terminus while GD interacts with a secondary site either on the channel itself or elsewhere.

sub-cellular localizations, affording a degree of spatial selectivity that is difficult to achieve with small molecules.[8,23,24,47] The prospect of engineering channel isoform selectivity into genetically encoded Ca_V channel blockers is intriguing and could potentially help address difficulties in developing selective small molecule blockers for specific Ca_V channel isoforms.[48,49]

What is the mechanism underlying ABD $Ca_V1.2$ inhibition by Rem? We previously showed that Rem inhibits recombinant wt α_{1C}/β_{2a} channels using at least 3 distinct mechanisms: (1) by reducing the number of channels at the cell surface; or by reducing the open probability (P_o) of surface channels in 2 distinguishable ways— (2) without an impact on voltage sensor movement (no effect on gating charge); (3) by partially immobilizing α_{1C} voltage sensors (reduced gating charge).[32] In mutant α_{1C}/β_{2aTM} channels, 2 of the mechanistic signatures of Rem inhibition (decreased channel surface density and reduced P_o without an impact on voltage sensors) but not the third (reduced P_o by voltage sensor immobilization) were eliminated. These previous results suggest that ABD inhibition by Rem is due to a reduced P_o of surface channels mediated by a partial immobilization of α_{1C} voltage sensor(s). Given the continuity between α_{1C}NT and the domain I (DI) S1-S4 voltage sensor it is tempting to speculate based on the "cross-linking model" we propose wherein Rem_{DCT} binds α_{1C}NT while the G-domain binds to a second site, that Rem impedes movement of at least the α_{1C} DI voltage sensor. Voltage clamp fluorimetry experiments could be used to directly test how and which of the 4 α_{1C} voltage sensors are affected by Rem.[50]

Our findings add to a growing list of molecules regulating the gating of Ca_V1 and Ca_V2 channels by targeting the N-termini of pore-forming α_1-subunits. These include reports that the α_{1B} N-terminus acts as a gated module that enables voltage-dependent G-protein $\beta\gamma$ subunit inhibition of $Ca_V2.2$ channels;[51] a role for α_{1C} N-terminus in protein kinase C modulation of $Ca_V1.2$ channels;[52,53] that the N-termini of $Ca_V1.2$ and $Ca_V1.3$ channels contains a Ca^{2+}-CaM binding site (termed NSCaTE for N-terminal spatial Ca^{2+} transforming element) that controls local vs. global spatial Ca^{2+} selectivity for CaM regulation of Ca_V channels;[54,55] and that deleting segments of α_{1C} N-terminus increases $I_{Ca,L}$ by enhancing channel P_o.[52,56]

Some aspects of our findings contrast with previous reports. While we found that Rem_{DCT} is necessary for $Ca_V1.2$ inhibition, a $Rem_{224–297}$ peptide that contained this whole region was not sufficient to block $I_{Ca,L}$. This result is in agreement with previous observations that a peptide comprising the Rem distal C-terminus alone ($Rem_{266–297}$) did not inhibit $Ca_V1.2$ channels reconstituted in tsA201 cells,[29] and that Rem2 C-terminus had no impact on endogenous $Ca_V2.2$ channels in SCG neurons.[30] By contrast, it was previously reported that $Gem_{223–296}$ (which lacks the Gem G-domain) was sufficient to bind auxiliary $Ca_V\beta$ and strongly inhibit recombinant $Ca_V2.1$ channels reconstituted in *Xenopus* oocytes.[44] Further, a different study showed that a 12 amino acid peptide derived from Gem C-terminus is also sufficient to inhibit $Ca_V2.1$ channels in excised patches from *Xenopus* oocytes.[57] These seemingly conflicting results could be due to differences in experimental techniques, cell systems, or simply the result of an emerging pattern of distinct mechanistic differences among RGK proteins with regard to the Ca_V channels inhibition. However, we found that CFP-$Gem_{223–296}$ did not bind $Ca_V\beta$ or inhibit either $Ca_V1.2$ or $Ca_V2.1$ channels reconstituted in HEK293 cells (Fig. S3).

Recently, Beqollari et al. (2014) found that while both Rad and Rem overexpressed in adult mice flexor digitorum brevis fibers potently inhibited endogenous $Ca_V1.1$ currents, only Rad also reduced $Ca_V1.1$ Vage sensor movement.[58] This is in contrast to cultured skeletal myotubes where Rem inhibited endogenous $Ca_V1.1$ current concomitantly with a reduction in gating charge.[59] Chimeric Rad/Rem analyses indicated that the N-terminus of Rad was necessary for the reduced $Ca_V1.1$ Vage-sensor movement in adult skeletal muscle fibers. Overall, taken together with these and other previous reports, our results add to a growing awareness that RGK inhibition of Ca_V channels is underlain by a rich variety of determinants and mechanisms that are specific for the RGK subtype, Ca_V1/Ca_V2 channel isoforms, and the cell context.[15]

Materials and methods

Molecular biology

To generate cyan fluorescent protein (CFP)-tagged RGK constructs [mouse Rem (NM_009047); human Gem (NM_181702)] we first cloned CFP into pcDNA4.1 (Invitrogen) using *KpnI* and *BamHI* sites. Subsequently, Rem and Gem cDNA were amplified using polymerase chain reaction (PCR) and cloned downstream of CFP using *BamHI* and *EcoRI* sites. To generate yellow fluorescent protein (YFP)-tagged $Ca_V\beta_{2a}$, we PCR amplified and cloned YFP into pAd CMV vector using *BamHI* and *XbaI* sites. $Ca_V\beta_{2a}$ was amplified by PCR and cloned upstream of YFP using *NheI* and *BamHI* sites. To generate YFP-tagged $Ca_V\beta_3$ we first cloned YFP into pcDNA3 using *KpnI* and *BamHI* sites. Subsequently, $Ca_V\beta_3$ was amplified downstream of YFP using *BamHI* and *Xba* sites. Point mutations in $Ca_V\beta$ were generated using QuikChange Site-Directed Mutagenesis Kit (Stratagene). PCR amplification and cloning was used to generate truncated Rem_{275} and Rem_{285} using *BamHI* and *EcoRI* sites. Chimeric RGK proteins were generated using overlap-extension PCR amplification and cloned into pcDNA4.1 (Invitrogen). All constructs were verified by sequencing.

Cell culture and transfection

HEK293 cells were maintained in DMEM supplemented with 10% FBS and 100 μg ml^{-1} penicillin-streptomycin. For electrophysiology experiments, HEK293 cells cultured in 35-mm tissue culture dishes were transiently transfected with α_{1C} (4 μg), β_{2a} (3 μg), T-antigen (2 μg) and the appropriate Rem, Gem or chimeric RGK construct (3 μg) using the calcium phosphate precipitation method. Cells were washed with PBS 4–6 h after transfection and maintained in supplemented DMEM. For confocal microscopy and FRET imaging experiments, transfected

HEK293 cells were replated onto 35-mm fibronectin-coated No. 0 glass bottom culture dishes (MatTek). For electrophysiology experiments, cells were replated onto fibronectin-coated glass coverslips 24–48 h after transfection.

Generation of adenoviruses

Rem-IRES-mCherry adenoviral vectors were generated using the Adeno-X CMV vector kit (Clontech). CFP-tagged adenoviral vectors were generated using the AdEasy XL Adenoviral Vector System (Agilent Technologies) as previously described.[31] The cDNA sequence comprising α_{1C}NT (residues 1–153) and II-III intracellular loop (residues 800–942) were amplified using PCR and spliced in-frame downstream of CFP using overlap extension PCR. The whole cDNA cassette comprising either CFP-α_{1C}NT or CFP-α_{1C} II-III loop was cloned into pShuttle for construction of adenoviral vectors using the AdEasy system.

Adult rat ventricular myocyte culture and infection

Primary cultures of adult rat heart ventricular myocytes were prepared as previously described,[60,61] and in accordance with the guidelines of the Columbia University Animal Care and Use Committee. Briefly, male Sprague-Dawley rats (Harlan) were euthanized with an overdose of halothane. Hearts were excised and ventricular myocytes isolated by enzymatic digestion with 1.7 mg Liberase-TM enzyme mix (Roche) using a Langendorff perfusion apparatus. Myocytes were cultured on laminin-coated glass coverslips (for electrophysiology experiments) or MatTek dishes (for confocal imaging experiments) in Medium 199 (Life Technologies) supplemented with (in mM): 5 carnitine, 5 creatine, 5 taurine, 0.5% penicillin-streptomycin-glutamine (Life Technologies), and 5% (vol/vol) FBS (Life Technologies). Cells were infected with 10–20 μL of viral stock in a final volume of 1–2 mL.

Electrophysiology

Whole-cell recordings on HEK293 cells were conducted 48–72 h after transfection at room temperature using an EPC-8 or EPC-10 patch clamp amplifier controlled by PULSE software (HEKA). Micropipettes were fashioned from 1.5 mm thin-walled glass with filament (World Precision Instruments). Series resistance was typically 1.7–2.5 MΩ. Internal solution contained (in mM): 135 cesium methanesulphonate ($MeSO_3$), 5 cesium chloride, 5 EGTA, 1 $MgCl_2$, 10 HEPES and 4 MgATP added fresh (pH 7.3). External solution contained (in mM): 140 tetraethylammonium-$MeSO_3$, 5 $BaCl_2$ and 10 HEPES (pH 7.3). Whole-cell *I-V* curves were generated from a family of step depolarizations (−50 to +70 mV from a holding potential of −90 mV). Currents were sampled at 25 kHz and filtered at 10 kHz. Traces were acquired at a repetition interval of 6 s. Leak and capacitive currents were subtracted using a P/8 protocol.

Whole-cell recordings of cultured rat ventricular myocytes were conducted at room temperature. Patch pipettes used typically had 1–2 MΩ series resistance when filled with internal solution containing (in mM): 150 cesium-methanesulfonate, 10 EGTA, 5 CsCl, 1$MgCl_2$, 10 HEPES and 4 MgATP added fresh (pH 7.3). Cells were perfused with normal Tyrode external solution during formation of gigaohm seal. Tyrode external solution contained (in mM): 138 NaCl, 4KCl, 2 $CaCl_2$, 1 MgCl2, 0.33 NaH_2PO_4, 10 HEPES (pH 7.4). After successful break-in to the whole-cell configuration the perfusing medium was switched to an external recording solution containing (in mM): 155 N-methy-D-glucamine-aspartate, 10 4-aminopyridine, 1 $MgCl_2$, 5 $BaCl_2$, 10 HEPES (pH 7.4). Currents were sampled at 50 KHz and filtered at 5 KHz and leak and capacitive currents were subtracted using a P/8 protocol.

Immunoprecipitation and Western blotting

Confluent cultures of HEK293 cells plated in 60-mm tissue culture dishes were harvested 48 h after transfection. Cells were washed in PBS and resuspended in 0.5 mL cold lysis buffer (50 mmol/L Tris-HCl, 150 mmol/L NaCl, 1% NP-40) containing protease inhibitor cocktail for 30 minutes. Cell lysates were centrifuged at 10,000 × g for 15 minutes at 4°C, and the supernatant precleared by incubation with 30 μL protein G beads slurry for 1 h. The mixture was centrifuged and the resulting supernatant incubated with 4 μg anti-Rem (SC58472, Santa Cruz) antibody and 30 μL protein G slurry for 1 h on a rotator. The mixture was again centrifuged, and the pellet washed 4 times with lysis buffer. 50 μL Laemmli sample buffer was added to the bead pellet and the mixture vortexed and heated (95°C for 10 minutes). The sample was centrifuged and the supernatant loaded onto a gel for subsequent SDS-PAGE and Western blot analyses.

For immunoblots, primary antibodies to GFP (Invitrogen, A6455) were detected by horse-radish peroxidase-conjugated secondary antibodies (goat-anti rabbit obtained from Thermo Scientific, 32260) and enhanced chemiluminescence (Thermo Scientific, 34080).

Confocal imaging

Static images of HEK 293 and cultured rat ventricular myocytes cells expressing CFP- and YFP-tagged proteins were imaged using a Leica TCS SP2 AOBS MP Confocal microscope with a 40 × oil objective (HCX PL APO 1.25–.75 NA). 458/514 nm argon laser line was used for excitation of fluorescent protein-tagged constructs.

FRET imaging

Three-cube FRET assay with CFP- (donor) and YFP-tagged (acceptor) molecules was used to probe specific protein-protein interactions in live cells as previously described.[39-41,62] Fluorescence images were acquired using a 40x oil objective (NA 1.3) on a Nikon Eclipse Ti-U inverted microscope fitted with an electron-multiplying CCD camera (QuantEM:512SC, Photometrics). Excitation wavelengths of 440 nm (CFP and FRET cubes) and 500 nm (YFP cube) were applied using a random access monochromator with a 75 W Xenon Arc lamp housing (PTI DeltaRam X, Photon Technology International). FRET efficiency was measured by acquiring 3 separate signals for each donor-acceptor pair condition: the donor channel (DD) which excites and detects donor emission, the acceptor channel (AA) which excites and detects acceptor emission, and the FRET channel (DA) which excites the donor and detects acceptor emission. The filter cubes used were (dichroic, emission): DD (455DCLP, D480/30M); AA (525DRLP, 530EFLP); DA (455DRLP, 535DF25). Cross-talk parameters were determined by imaging cells expressing either donor (CFP) or acceptor (YFP) fluorescent proteins alone. To avoid outlying data points only donor/acceptor ratios from 0.1 to 6 and signal/noise ratios with a minimum of 2 were used for FRET efficiency calculations. FRET efficiency and relative donor and acceptor concentrations were calculated as described.[40,41,62]

Data and statistical analyses

Data were analyzed off-line using PulseFit (HEKA), Microsoft Excel and Origin software. Data were plotted and statistical analyses were performed in Origin using built-in functions. Statistically significant differences between means ($P < 0.05$) were determined using one-way ANOVA followed by Bonferroni post hoc analyses for comparisons involving more than 2 groups. Data are represented as means ± SEM.

Disclosure of potential conflicts of interest

No potential conflicts of interest were disclosed.

Acknowledgments

We thank Ming Chen for technical assistance and members of the Colecraft lab for helpful discussions.

Funding

This research was supported by a grant from the National Institutes of Health (R01 GM107585 to HMC); an AHA pre-doctoral fellowship (13PRE13970018 to AAP), a UNCF-Merck graduate dissertation fellowship (CU11-2479 to AAP), and an American Heart Association Established Investigator Award (HMC).

References

[1] Hille B. Ion Channels of Excitable Membranes. Sunderland: Sinauer Associates, Inc., 2001
[2] Catterall WA. Structure and regulation of voltage-gated Ca^{2+} channels. Annu Rev Cell Dev Biol 2000; 16:521-55; PMID:11031246; http://dx.doi.org/10.1146/annurev.cellbio.16.1.521
[3] Simms BA, Zamponi GW. Neuronal voltage-gated calcium channels: structure, function, and dysfunction. Neuron 2014; 82:24-45; PMID:24698266; http://dx.doi.org/10.1016/j.neuron.2014.03.016
[4] Buraei Z, Yang J. The {beta} Subunit of Voltage-Gated Ca2+ Channels. Physiol Rev 2010; 90:1461-506; PMID:20959621; http://dx.doi.org/10.1152/physrev.00057.2009
[5] Dolphin AC. Beta subunits of voltage-gated calcium channels. J Bioenerg Biomembr 2003; 35:599-620; PMID:15000522; http://dx.doi.org/10.1023/B:JOBB.0000008026.37790.5a
[6] Neely A, Hidalgo P. Structure-function of proteins interacting with the alpha1 pore-forming subunit of high-voltage-activated calcium channels. Frontiers in physiology 2014; 5:209; PMID:24917826; http://dx.doi.org/10.3389/fphys.2014.00209
[7] Ben-Johny M, Yue DT. Calmodulin regulation (calmodulation) of voltage-gated calcium channels. J Gen Physiol 2014; 143:679-92; PMID:24863929; http://dx.doi.org/10.1085/jgp.201311153

[8] Xu X, Colecraft HM. Engineering proteins for custom inhibition of Ca(V) channels. Physiology (Bethesda) 2009; 24:210-8; PMID:19675352; http://dx.doi.org/10.1152/physiol.00010.2009
[9] Striessnig J. Pharmacology, structure and function of cardiac L-type Ca(2+) channels. Cell Physiol Biochem 1999; 9:242-69; PMID:10575201; http://dx.doi.org/10.1159/000016320
[10] Surmeier DJ, Schumacker PT. Calcium, bioenergetics, and neuronal vulnerability in Parkinson's disease. J Biol Chem 2013; 288:10736-41; PMID:23086948; http://dx.doi.org/10.1074/jbc.R112.410530
[11] Triggle DJ. Calcium channel antagonists: clinical uses–past, present and future. Biochem Pharmacol 2007; 74:1-9; PMID:17276408; http://dx.doi.org/10.1016/j.bcp.2007.01.016
[12] Kochegarov AA. Pharmacological modulators of voltage-gated calcium channels and their therapeutical application. Cell Calcium 2003; 33:145-62; PMID:12600802; http://dx.doi.org/10.1016/S0143-4160(02)00239-7
[13] Beguin P, Nagashima K, Gonoi T, Shibasaki T, Takahashi K, Kashima Y, Ozaki N, Geering K, Iwanaga T, Seino S. Regulation of Ca2+ channel expression at the cell surface by the small G-protein kir/Gem. Nature 2001; 411:701-6; PMID:11395774; http://dx.doi.org/10.1038/35079621
[14] Finlin BS, Crump SM, Satin J, Andres DA. Regulation of voltage-gated calcium channel activity by the Rem and Rad GTPases. Proc Natl Acad Sci U S A 2003; 100:14469-74; PMID:14623965; http://dx.doi.org/10.1073/pnas.2437756100
[15] Yang T, Colecraft HM. Regulation of voltage-dependent calcium channels by RGK proteins. Biochim Biophys Acta 2013; 1828:1644-54; PMID:23063948; http://dx.doi.org/10.1016/j.bbamem.2012.10.005
[16] Flynn R, Zamponi GW. Regulation of calcium channels by RGK proteins. Channels (Austin) 2010; 4:434-9; PMID:20953143; http://dx.doi.org/10.4161/chan.4.6.12865
[17] Maguire J, Santoro T, Jensen P, Siebenlist U, Yewdell J, Kelly K. Gem: an induced, immediate early protein belonging to the Ras family. Science 1994; 265:241-4; PMID:7912851; http://dx.doi.org/10.1126/science.7912851
[18] Reynet C, Kahn CR. Rad: a member of the Ras family overexpressed in muscle of type II diabetic humans. Science 1993; 262:1441-4; PMID:8248782; http://dx.doi.org/10.1126/science.8248782
[19] Finlin BS, Andres DA. Rem is a new member of the Rad- and Gem/Kir Ras-related GTP-binding protein family repressed by lipopolysaccharide stimulation. J Biol Chem 1997; 272:21982-8; PMID:9268335; http://dx.doi.org/10.1074/jbc.272.35.21982
[20] Chang L, Zhang J, Tseng YH, Xie CQ, Ilany J, Bruning JC, Sun Z, Zhu X, Cui T, Youker KA, et al. Rad GTPase deficiency leads to cardiac hypertrophy. Circulation 2007; 116:2976-83; PMID:18056528; http://dx.doi.org/10.1161/CIRCULATIONAHA.107.707257
[21] Magyar J, Kiper CE, Sievert G, Cai W, Shi GX, Crump SM, Li L, Niederer S, Smith N, Andres DA, et al. Rem-GTPase regulates cardiac myocyte L-type calcium current. Channels (Austin) 2012; 6:166-73; PMID:22854599; http://dx.doi.org/10.4161/chan.20192
[22] Gunton JE, Sisavanh M, Stokes RA, Satin J, Satin LS, Zhang M, Liu SM, Cai W, Cheng K, Cooney GJ, et al. Mice Deficient in GEM GTPase Show Abnormal Glucose Homeostasis Due to Defects in Beta-Cell Calcium Handling. PLoS One 2012; 7:e39462; PMID:22761801; http://dx.doi.org/10.1371/journal.pone.0039462
[23] Murata M, Cingolani E, McDonald AD, Donahue JK, Marban E. Creation of a genetic calcium channel blocker by targeted gem gene transfer in the heart. Circ Res 2004; 95:398-405; PMID:15242970; http://dx.doi.org/10.1161/01.RES.0000138449.85324.c5
[24] Makarewich CA, Correll RN, Gao H, Zhang H, Yang B, Berretta RM, Rizzo V, Molkentin JD, Houser SR. A caveolae-targeted L-type Ca(2)+ channel antagonist inhibits hypertrophic signaling without reducing cardiac contractility. Circ Res 2012; 110:669-74; PMID:22302787; http://dx.doi.org/10.1161/CIRCRESAHA.111.264028
[25] Beguin P, Ng YJ, Krause C, Mahalakshmi RN, Ng MY, Hunziker W. RGK small GTP-binding proteins interact with the nucleotide kinase domain of Ca2+-channel beta-subunits via an uncommon effector binding domain. J Biol Chem 2007; 282:11509-20; PMID:17303572; http://dx.doi.org/10.1074/jbc.M606423200
[26] Yang T, Puckerin A, Colecraft HM. Distinct RGK GTPases Differentially Use alpha(1)- and Auxiliary beta-Binding-Dependent Mechanisms to Inhibit Ca(V)1.2/Ca(V)2.2 Channels. PLoS One 2012; 7:e37079; PMID:22590648; http://dx.doi.org/10.1371/journal.pone.0037079
[27] Yang T, He LL, Chen M, Fang K, Colecraft HM. Bio-inspired voltage-dependent calcium channel blockers. Nat Commun 2013; 4:2540; PMID:24096474
[28] Yang T, Suhail Y, Dalton S, Kernan T, Colecraft HM. Genetically encoded molecules for inducibly inactivating CaV channels. Nat Chem Biol 2007; 3:795-804; PMID:17952065; http://dx.doi.org/10.1038/nchembio.2007.42
[29] Correll RN, Pang C, Finlin BS, Dailey AM, Satin J, Andres DA. Plasma membrane targeting is essential for Rem-mediated Ca2+ channel inhibition. J Biol Chem 2007; 282:28431-40; PMID:17686775; http://dx.doi.org/10.1074/jbc.M706176200
[30] Chen H, Puhl HL, 3rd, Niu SL, Mitchell DC, Ikeda SR. Expression of Rem2, an RGK family small GTPase, reduces N-type calcium current without affecting channel surface density. J Neurosci 2005; 25:9762-72; PMID:16237180; http://dx.doi.org/10.1523/JNEUROSCI.3111-05.2005
[31] Xu X, Marx SO, Colecraft HM. Molecular mechanisms, and selective pharmacological rescue, of Rem-inhibited CaV1.2 channels in heart. Circ Res 2010; 107:620-30; PMID:20616312; http://dx.doi.org/10.1161/CIRCRESAHA.110.224717
[32] Yang T, Xu X, Kernan T, Wu V, Colecraft HM. Rem, a member of the RGK GTPases, inhibits recombinant CaV1.2 channels using multiple mechanisms that require distinct conformations of the GTPase. J Physiol 2010;

588:1665-81; PMID:20308247; http://dx.doi.org/10.1113/jphysiol.2010.187203
[33] Wang G, Zhu X, Xie W, Han P, Li K, Sun Z, Wang Y, Chen C, Song R, Cao C, et al. Rad as a novel regulator of excitation-contraction coupling and beta-adrenergic signaling in heart. Circ Res 2010; 106:317-27; PMID:19926875; http://dx.doi.org/10.1161/CIRCRESAHA.109.208272
[34] Finlin BS, Mosley AL, Crump SM, Correll RN, Ozcan S, Satin J, Andres DA. Regulation of L-type Ca2+ channel activity and insulin secretion by the Rem2 GTPase. J Biol Chem 2005; 280:41864-71; PMID:15728182; http://dx.doi.org/10.1074/jbc.M414261200
[35] Jhun BS, J OU, Wang W, Ha CH, Zhao J, Kim JY, Wong C, Dirksen RT, Lopes CM, Jin ZG. Adrenergic signaling controls RGK-dependent trafficking of cardiac voltage-gated L-type Ca2+ channels through PKD1. Circ Res 2012; 110:59-70; PMID:22076634; http://dx.doi.org/10.1161/CIRCRESAHA.111.254672
[36] Colicelli J. Human RAS superfamily proteins and related GTPases. Sci STKE 2004; 2004:RE13; PMID:15367757
[37] Sprang SR. G protein mechanisms: insights from structural analysis. Annu Rev Biochem 1997; 66:639-78; PMID:9242920; http://dx.doi.org/10.1146/annurev.biochem.66.1.639
[38] Sasson Y, Navon-Perry L, Huppert D, Hirsch JA. RGK family G-domain:GTP analog complex structures and nucleotide-binding properties. J Mol Biol 2011; 413:372-89; PMID:21903096; http://dx.doi.org/10.1016/j.jmb.2011.08.017
[39] Erickson MG, Alseikhan BA, Peterson BZ, Yue DT. Preassociation of calmodulin with voltage-gated Ca(2+) channels revealed by FRET in single living cells. Neuron 2001; 31:973-85; PMID:11580897; http://dx.doi.org/10.1016/S0896-6273(01)00438-X
[40] Chen H, Puhl HL, 3rd, Ikeda SR. Estimating protein-protein interaction affinity in living cells using quantitative Forster resonance energy transfer measurements. J Biomed Opt 2007; 12:054011; PMID:17994899; http://dx.doi.org/10.1117/1.2799171
[41] Chen H, Puhl HL, 3rd, Koushik SV, Vogel SS, Ikeda SR. Measurement of FRET efficiency and ratio of donor to acceptor concentration in living cells. Biophys J 2006; 91: L39-41; PMID:16815904; http://dx.doi.org/10.1529/biophysj.106.088773
[42] Crabtree GR, Schreiber SL. Three-part inventions: intracellular signaling and induced proximity. Trends Biochem Sci 1996; 21:418-22; PMID:8987395; http://dx.doi.org/10.1016/S0968-0004(96)20027-1
[43] Inoue T, Heo WD, Grimley JS, Wandless TJ, Meyer T. An inducible translocation strategy to rapidly activate and inhibit small GTPase signaling pathways. Nat Methods 2005; 2:415-8; PMID:15908919; http://dx.doi.org/10.1038/nmeth763
[44] Leyris JP, Gondeau C, Charnet A, Delattre C, Rousset M, Cens T, Charnet P. RGK GTPase-dependent CaV2.1 Ca2+ channel inhibition is independent of CaVbeta-subunit-induced current potentiation. FASEB J 2009; 23:2627-38; PMID:19332647; http://dx.doi.org/10.1096/fj.08-122135
[45] Correll RN, Pang C, Niedowicz DM, Finlin BS, Andres DA. The RGK family of GTP-binding proteins: regulators of voltage-dependent calcium channels and cytoskeleton remodeling. Cell Signal 2008; 20:292-300; PMID:18042346; http://dx.doi.org/10.1016/j.cellsig.2007.10.028
[46] Heo WD, Inoue T, Park WS, Kim ML, Park BO, Wandless TJ, Meyer T. PI(3,4,5)P3 and PI(4,5)P2 lipids target proteins with polybasic clusters to the plasma membrane. Science 2006; 314:1458-61; PMID:17095657; http://dx.doi.org/10.1126/science.1134389
[47] Ibanez-Tallon I, Nitabach MN. Tethering toxins and peptide ligands for modulation of neuronal function. Curr Opin Neurobiol 2012; 22:72-8; PMID:22119144; http://dx.doi.org/10.1016/j.conb.2011.11.003
[48] Huang H, Ng CY, Yu D, Zhai J, Lam Y, Soong TW. Modest CaV1.342-selective inhibition by compound 8 is beta-subunit dependent. Nat Commun 2014; 5:4481; PMID:25057870
[49] Kang S, Cooper G, Dunne SF, Dusel B, Luan CH, Surmeier DJ, Silverman RB. CaV1.3-selective L-type calcium channel antagonists as potential new therapeutics for Parkinson's disease. Nat Commun 2012; 3:1146; PMID:23093183; http://dx.doi.org/10.1038/ncomms2149
[50] Pantazis A, Savalli N, Sigg D, Neely A, Olcese R. Functional heterogeneity of the four voltage sensors of a human L-type calcium channel. Proc Natl Acad Sci U S A 2014; 111:18381-6; PMID:25489110; http://dx.doi.org/10.1073/pnas.1411127112
[51] Agler HL, Evans J, Tay LH, Anderson MJ, Colecraft HM, Yue DT. G protein-gated inhibitory module of N-type (ca(v) 2.2) ca2+ channels. Neuron 2005; 46:891-904; PMID:15953418; http://dx.doi.org/10.1016/j.neuron.2005.05.011
[52] Shistik E, Ivanina T, Blumenstein Y, Dascal N. Crucial role of N terminus in function of cardiac L-type Ca2+ channel and its modulation by protein kinase C. J Biol Chem 1998; 273:17901-9; PMID:9651396; http://dx.doi.org/10.1074/jbc.273.28.17901
[53] McHugh D, Sharp EM, Scheuer T, Catterall WA. Inhibition of cardiac L-type calcium channels by protein kinase C phosphorylation of two sites in the N-terminal domain. Proc Natl Acad Sci U S A 2000; 97:12334-8; PMID:11035786; http://dx.doi.org/10.1073/pnas.210384297
[54] Dick IE, Tadross MR, Liang H, Tay LH, Yang W, Yue DT. A modular switch for spatial Ca2+ selectivity in the calmodulin regulation of CaV channels. Nature 2008; 451:830-4; PMID:18235447; http://dx.doi.org/10.1038/nature06529
[55] Tadross MR, Dick IE, Yue DT. Mechanism of local and global Ca2+ sensing by calmodulin in complex with a Ca2+ channel. Cell 2008; 133:1228-40; PMID:18585356; http://dx.doi.org/10.1016/j.cell.2008.05.025
[56] Wei X, Neely A, Olcese R, Lang W, Stefani E, Birnbaumer L. Increase in Ca2+ channel expression by deletions at

the amino terminus of the cardiac alpha 1C subunit. Receptors Channels 1996; 4:205-15; PMID:9065969

[57] Fan M, Zhang WK, Buraei Z, Yang J. Molecular Determinants of Gem Protein Inhibition of P/Q-type Ca2+ Channels. J Biol Chem 2012; 287:22749-58; PMID:22589533; http://dx.doi.org/10.1074/jbc.M111.291872

[58] Beqollari D, Romberg CF, Meza U, Papadopoulos S, Bannister RA. Differential effects of RGK proteins on L-type channel function in adult mouse skeletal muscle. Biophys J 2014; 106:1950-7; PMID:24806927; http://dx.doi.org/10.1016/j.bpj.2014.03.033

[59] Bannister RA, Colecraft HM, Beam KG. Rem inhibits skeletal muscle EC coupling by reducing the number of functional L-type Ca2+ channels. Biophys J 2008; 94:2631-8; PMID:18192376; http://dx.doi.org/10.1529/biophysj.107.116467

[60] Colecraft HM, Alseikhan B, Takahashi SX, Chaudhuri D, Mittman S, Yegnasubramanian V, Alvania RS, Johns DC, Marbán E, Yue DT. Novel functional properties of Ca^{2+} channel beta subunits revealed by their expression in adult rat heart cells. J Physiol 2002; 541:435-52; PMID:12042350; http://dx.doi.org/10.1113/jphysiol.2002.018515

[61] Subramanyam P, Chang DD, Fang K, Xie W, Marks AR, Colecraft HM. Manipulating L-type calcium channels in cardiomyocytes using split-intein protein transsplicing. Proc Natl Acad Sci U S A 2013; 110:15461-6; PMID:24003157; http://dx.doi.org/10.1073/pnas.1308161110

[62] Chang DD, Colecraft HM. Rad and Rem are non-canonical G-proteins with respect to the regulatory role of guanine nucleotide binding in Ca(V)1.2 channel regulation. J Physiol 2015; 593:5075-90; PMID:26426338; http://dx.doi.org/10.1113/JP270889